Simple and Causal Copper Cable Model Suitable for G.fast Frequencies

6 authors, including:

Chenguang Lu
Ericsson
31 PUBLICATIONS **62** CITATIONS

SEE PROFILE

Miguel Berg
Ericsson
28 PUBLICATIONS **255** CITATIONS

SEE PROFILE

Aldebaro Klautau
Federal University of Pará
110 PUBLICATIONS **1,381** CITATIONS

SEE PROFILE

Per Ola Börjesson
Lund University
100 PUBLICATIONS **7,390** CITATIONS

SEE PROFILE

Some of the authors of this publication are also working on these related projects:

Project   ECG signal processing View project

Project   Next generation Over-The-Top multimedia Services View project

Simple and Causal Copper Cable Model Suitable for G.fast Frequencies

Diogo Acatauassu, *Member, IEEE*, Stefan Höst, *Member, IEEE*, Chenguang Lu, Miguel Berg, *Member, IEEE*, Aldebaro Klautau, *Senior Member, IEEE*, and Per Ola Börjesson, *Senior Member, IEEE*

Abstract—G.fast is a new standard from the International Telecommunication Union, which targets 1 Gb/s over short copper loops using frequencies up to 212 MHz. This new technology requires accurate parametric cable models for simulation, design, and performance evaluation tests. Some existing copper cable models were designed for the very high speed digital subscriber line spectra, i.e., frequencies up to 30 MHz, and adopt assumptions that are violated when the frequency range is extended to G.fast frequencies. This paper introduces a simple and causal cable model that is able to accurately characterize copper loops composed by single or multiple segments, in both frequency and time domains. Results using G.fast topologies show that, apart from being accurate, the new model is attractive due to its low computational cost and closed-form expressions for fitting its parameters to measurement data.

Index Terms—Cable models, digital subscriber line (DSL), G.fast, transmission line theory, twisted-pair copper cables.

I. INTRODUCTION

OVER the last twenty years, the emergence of new digital services and applications has fueled the development of new broadband access technologies, capable of delivering the required data rates to the final customers. One broadband architecture is the fiber-to-the-home (FTTH) [1], which assumes taking fiber all the way to the customer. However, the final drop of 20–200 m is the most expensive part of the access section, typically meaning digging along individual paths to each customer. Furthermore, the cost of installing new fiber plant inside the customer's premises is higher than utilizing existing wires. If instead the final drop of the existing copper telephone grid is used to transmit the signals, these inconveniences and expenses can be avoided.

Due to the economic issues, the use of a *hybrid* copper and fiber architecture called fiber-to-the-distribution-point (FTTdp) is attractive in both fixed access and mobile backhauling scenarios. This trend led the industry and academia to start developing the fourth generation DSL broadband systems [2]. More specifically, since 2011 the International Telecommunication Union (ITU) is working on the G.fast standard [3]. The aim is to achieve 1 Gb/s from the last distribution point in the copper loop. To reach these data rates a bandwidth of around 100 or 200 MHz can be used. Because the signal attenuation over twisted-pairs increases with both frequency and cable length, G.fast is targeting loops not longer than 250 meters.

In this context, accurate models capable of describing the electrical characteristics of short twisted-pair cables operating at relatively high frequencies are key elements for simulation and performance evaluation tests of the G.fast systems. Most parametric cable models in the literature were designed for the VDSL spectra with a maximum bandwidth of 30 MHz [4]–[11]. More recently, new models targeting G.fast have been proposed [12]–[14]. In [12] a new class of parametric model called TNO2, suitable for time and frequency domain studies, was introduced. The model TNO/EAB in [13] is an extension of [12], which incorporates an extra parameter for improving the model accuracy. It was agreed by ITU that the TNO/EAB model should be used for characterizing typical aerial drop cables (e.g., CAD55 cables) that compose the G.fast wiring topologies and reference loops [15]. Beyond new models, adaptations on existing ones designed for xDSL bands have also been proposed. In [16], new parameter values were given for the well-known BT0 model, targeting frequencies up to hundreds of MHz.

The presented work extends [14], which proposed causal models for the propagation constant γ. The models in [14] aimed at single-gauge twisted-pairs with ideal terminations at both ends and could not be used, for example, for modeling multiple segments connected in cascade or topologies with bridged-taps. Here, a simple and causal model for the characteristic impedance Z_0, called HM1, is derived. Together with the so-called KM1 γ model from [14], the new Z_0 model composes the KHM model, which supports multiple segments and frequencies up to hundreds of MHz, has few parameters, is causal and has a closed-form expression for fitting to measurement data.

The text is organized as follows. Section II gives a brief review of concepts about the transmission line theory and defines notation. Section III discusses and categorizes existing cable models, contextualizing the ones proposed by the authors of this work. Section IV reviews the adopted γ model and presents

TABLE I
SUMMARY OF EXISTING CABLE MODELS. "PHYS." IDENTIFIES A PHYSICAL MODEL AND "G.FAST f"
A MODEL DESIGNED TO BEHAVE WELL AT G.FAST FREQUENCIES ($f \in [2.2, 212]$ MHz)

Model	M	Γ	Phys.	Analysis $\hat{\Theta} = \mathcal{A}\{\Xi\}$	Criterion	G.fast f	Causal	Year
BT0 [4], [16]	11	$RLCG$	No	Closed-form, Iterative	LS, ML	No, Yes	No	1996, 2011
KPN1 [5]	11	Z, Y	No	Iterative	LS	No	No	1997
Whei's [20]	12	$RLCG$	No	Closed-form	LS	No	No	1997
MAR1 [7]	7	Z, Y	No	Iterative	ML	No	Yes	1998
Chen's [8]	3	γ	No	Closed-form	LS	No	No	1998
VUB1 [9]	6	Z, Y	Yes	Iterative	ML	No	Yes	2001
TIA/EIA [21]	3	α	No	Closed-form	LS	No	No	2001
CEI/IEC [22]	8	Z_0	No	Closed-form	LS	No	No	2002
VUB0 [10]	5	Z, Y	Yes	Iterative	ML	No	Yes	2002
BT0$_H$ [11]	4	$RLCG$	No	Closed-form	LS	No	Yes	2008
TNO2 [12]	9	Z, Y	No	Iterative	LS	Yes	Yes	2011
TNO/EAB [13]	10	Z, Y	No	Closed-form	LS	Yes	Yes	2012
KM1, KM2, KM3 [14]	3, 4, 5	γ	No	Closed-form	LS	Yes	Yes	2013
Proposed HM1	2	Z_0	No	Closed-form	LS	Yes	Yes	
Proposed KHM (KM1+HM1)	5	Z_0, γ	No	Closed-form	LS	Yes	Yes	

the new Z_0 model, together with the procedure for fitting the values of its parameters. Section V presents experimental results indicating that the KHM model is able to characterize generic copper loops with accuracy in both frequency and time domains. Both measured and simulated data were used in order to obtain the results. Some benchmarks in order to highlight the low computational cost of the model are also presented in this section. Section VI presents the conclusions.

II. BRIEF REVIEW OF TRANSMISSION LINE THEORY

According to the classical transmission line theory, e.g., [17], the electrical characteristics of twisted-pair copper cables are determined by the frequency dependent *primary coefficients*, the series resistance $R(f)$, series inductance $L(f)$, shunt conductance $G(f)$ and shunt capacitance $C(f)$. These coefficients compose the series impedance $Z(f) = R(f) + j2\pi f L(f)$ and shunt admittance $Y(f) = G(f) + j2\pi f C(f)$. From the primary coefficients, one can derive the *secondary coefficients*, the *characteristic impedance* and the *propagation constant*, as

$$Z_0(f) = \sqrt{\frac{Z(f)}{Y(f)}} \quad \text{and} \quad \gamma(f) = \sqrt{Z(f)Y(f)}, \quad (1)$$

respectively. Writing the propagation constant as a complex function we get

$$\gamma(f) = \alpha(f) + j\beta(f), \quad (2)$$

where $\alpha(f)$ is the *attenuation constant* and $\beta(f)$ the *phase constant*.

For the last drop of the telephony loop, or for mobile backhauling scenarios, one has topologies with a single cable segment and in these cases it suffices to have $\gamma(f)$ to obtain the *transfer function* of the loop $H(f)$. Assuming a perfectly-terminated[1] homogeneous[2] line, the transfer function becomes

$$H(f) = e^{-d\gamma(f)}. \quad (3)$$

However, for more complex cable scenarios containing multiple segments of distinct gauges, bridged-taps, etc, the classical *two-port network* modeling is used in order to construct an electrical equivalent described by the *ABCD matrices* obtained from the secondary coefficients of each segment.

The overall ABCD matrix to characterizes the topology is the product of the individual ABCD matrices of each segment. From the T_o matrix, it is possible to derive the transfer function of the loop based on the *insertion loss*[3] [8] given by

$$H(f) = \frac{Z_l + Z_s}{AZ_l + B + CZ_sZ_l + DZ_s}, \quad (4)$$

where Z_s and Z_l are the source and load impedances, respectively.

III. REVIEW OF EXISTING CABLE MODELS

Due to the renewed interest in copper cable modeling, it is timely to discuss in this section a taxonomy based on the most valued features of a model. Hence, a summary of cable models presented in the open literature is shown in Table I, with the highlighted features further discussed in the next subsections.

A. Parameters and Synthesis Equations

A cable model is assumed to be composed by a set $\Theta = \{\Theta_1, \ldots, \Theta_M\}$ of M parameters and an associated set $\Gamma = \{\Gamma_1, \ldots, \Gamma_N\}$ of N *synthesis* equations that are functions of the parameters Θ. For example, considering that Γ_1 estimates the resistance $R(f)$, it could be denoted as $R_\Theta(f)$. But for simplicity, it is denoted as R instead. Typically, $N = 1, 2$ or 4 and the synthesis equations describe the primary coefficients $\Gamma = \{R, L, G, C\}$, or the secondary coefficients, $\Gamma = \{Z_0, \gamma\}$. As previously discussed, if the application allows and (3) suffices, it is also possible to simply model the propagation constant and $\Gamma = \{\gamma\}$.

---

[1] A line terminated with its characteristic impedance.
[2] A line in which the electrical and magnetic properties of the medium surrounding the conductors are the same everywhere.

[3] The use of insertion loss for characterizing $H(f)$ is a common practice adopted by telecommunication engineers [8], [18], [19].

B. Nature of the Parameters

The cable model can be classified according to the nature of the parameters in Θ [23]. The model is called *physical* if all its parameters have a physical interpretation, such as the conductivity and permeability (which are related to the geometry and material of the metallic conductors). The model is classified as *empirical* if at least one of its parameters does not have a physical interpretation. Typically, extra empirical parameters are incorporated to achieve improved matching between the model results and actual measurements.

C. Analysis Procedure

For this work, it is convenient to consider that the full specification of a cable model also includes the description of the *analysis* procedure, which aims at obtaining an estimate $\hat{\Theta}$ of the parameters from given data Ξ and is generically denoted here by $\hat{\Theta} = \mathcal{A}\{\Xi\}$. The data Ξ can be obtained, for example, using specialized equipments such as vector network analyzers and impedance analyzers. The associated analysis can be done either via closed-form expressions of the type $\hat{\Theta}_i = f(\Xi)$ or iterative optimization in the fitting procedures such as Levenberg-Marquardt and genetic algorithms [24]. Two optimization criteria widely used in the analysis procedure are the *maximum likelihood* (ML) and *least-squares* (LS) [25].

D. Computational Cost

An interesting feature that a cable model may have is easiness of the associated analysis procedure. Depending on the application, the computational cost of the analysis may be negligible or not. An example of the first case is when the analysis is conducted off-line and is fast when contrasted to setting up and conducting the measurements to obtain Ξ. In contrast, the analysis may have to be executed in a real time application by a limited-power embedded system [26] or repeatedly invoked as part of an optimization process [27]. In cases of analysis-by-synthesis such as the genetic algorithm search proposed in [27], even the cost of the synthesis procedure is important, i.e., the simpler the N equations in Γ, the better.

Besides the advantage with respect to the computational cost, if a cable model allows the analysis to be done with closed-form expressions, it also facilitates the user interaction. When dealing with iterative optimization procedures, defining the search space and initial conditions may not be a trivial task [23]. A related aspect is that many iterative procedures can get stuck in a local maximum (or minimum) and do not guarantee convergence.

E. Support to Frequencies Around 200 MHz

As mentioned, many previous cable models are restricted to operating for example over the VDSL spectra (up to 30 MHz) [4]–[11] and do not take into account effects that occur at higher frequencies. When considering G.fast frequencies, it has been seen, e.g., [12], [13], [16], [28], that the direct extrapolation of

previous models does not lead to a reliable model if neglecting the effects of the dielectric losses, which is now important, or assume that the shunt conductance is zero. Hence, Table I distinguishes the models that were specifically designed to support frequencies from 2.2 up to 212 MHz.

F. Causality

The causality of the system generated by a given model can be inferred from the *impulse response*, $h(t) = \mathcal{F}^{-1}\{H(f)\}$ and the *propagation delay* $T_{pd} = d/s$, where s is the wave propagation velocity. A system where the impulse response has significant energy during the propagation delay is considered to be non-causal.

It should be noted that some classical cable models can exhibit non-causal behavior in time-domain since they violate the Hilbert transform relations between the real and imaginary parts in the frequency-domain [29]. In some situations this is not a problem. Many important results can be obtained via frequency-domain simulations, such as bit rate estimates via channel capacity equations that depend on power spectral densities and the channel transfer function. However, in other cases, e.g., evaluation of the cyclic-prefix duration [30], non-causal models should be avoided given that they can hinder the results interpretation.

G. Crosstalk Modeling

It is important to emphasize that the parametric models described in Table I, as well as the ones proposed by the authors of this work, focus on characterizing direct transmission channels, and not crosstalk channels. The behavior over frequency for the crosstalk channels is quite different from the one observed for the direct path. Here, for completeness, some pointers to crosstalk channel modeling are provided in the sequel but the scope of the paper are models for the direct channels.

Because of the variability of crosstalk coupling functions, crosstalk is commonly characterized by either stochastic models, which provide distinct realizations of crosstalk channels, or worst-case models. For example, a 1% worst-case FEXT (far-end crosstalk) model predicts that no more than one percent of all FEXT transfer functions in the cable will be more severe than the one derived by the model, as discussed in [19], [31]–[34].

Stochastic crosstalk models have been proposed in [35], [36], for better modeling the amplitude and phase variations of the crosstalk coupling functions, aiming at applications that require a set of distinct crosstalk channels. It should be noted that the stochastic models presented in [35], [36] were developed (and evaluated) for characterizing crosstalk at VDSL2 frequencies. Crosstalk models that focus on frequencies up to hundreds of MHz are the FEXT models discussed in [37], [38].

The next section presents a new model for the direct channel via γ and Z_0. It has only five empirical parameters that allow closed-form expressions during the analysis procedure and lead to causal systems.

IV. THE PROPOSED KHM CABLE MODEL

Recently, a new model for the propagation constant γ was proposed by the authors [14]. This model is described and then the proposed model for Z_0 is presented, followed by its fitting procedure.

A. The Propagation Constant

In [14] three versions of the propagation constant model were suggested; KM1, KM2, and KM3. In this work, only the first model (KM1) will be used. KM2 and KM3 can also be utilized in a similar manner, but the evidence from the experiments is that KM1 is accurate enough for the investigated topologies.

Definition 1: The propagation constant, $\gamma = \alpha + j\beta$, is modeled by

$$\alpha = k_1 \sqrt{f} + k_2 f \tag{5}$$

$$\beta = k_1 \sqrt{f} - k_2 \frac{2}{\pi} f \ln f + k_3 f. \tag{6}$$

□

The next subsection presents a model for Z_0, which together with KM1 will allow modeling complex scenarios containing multiple segments of distinct gauges and bridged-taps, for example.

B. Proposed Model for the Characteristic Impedance

The Z_0 function describes the instantaneous impedance that a signal will see as it propagates along the line. Twisted-pair copper cables typically adopted by high-speed data transmission technologies are made with 18 to 26 American gauge wire, and with the typical insulation thickness, the characteristic impedance is approximately 100 to 130 Ohms [39].

From (1),

$$Z_0(f) = \sqrt{\frac{R(f) + j\omega L(f)}{G(f) + j\omega C(f)}}, \tag{7}$$

where $\omega = 2\pi f$. As in the above equation, the dependence on f will be made explicit when it helps to avoid confusion with dependence on ω.

The HM1 model for Z_0 is derived following procedures that are similar to the ones described in [14]. We will use a generalized version of the *series resistance* and *series inductance* from the $BT0_H$ model [11], which are defined as

$$R(f) = R_0 Q\left(\frac{f}{v}\right) \quad \text{and} \quad L(f) = \frac{R_0}{2\pi f} \Lambda\left(\frac{f}{v}\right) + L_\infty, \tag{8}$$

where

$$Q(\phi) = \sqrt[4]{1 + \phi^2} \tag{9}$$

and $\Lambda(\eta)$ is the Hilbert transform of $Q(\phi)$

$$\Lambda(\eta) = -\frac{1}{\pi} \int_{\mathbb{R}} \frac{Q(\phi)}{\eta - \phi} d\phi. \tag{10}$$

Another adopted expression is the generalized version of the *shunt capacitance* and *shunt conductance* from [14], which are given by

$$G(f) = G_0 |f|, \tag{11}$$

and

$$C(f) = G_0 \frac{2}{\pi} \left(1 - \ln|2\pi f|\right) + C_\infty. \tag{12}$$

The derivation is then based on a series expansion of Z_0. Rewriting (7), one gets

$$Z_0 = \sqrt{\frac{j\omega L \left(1 + \frac{R}{j\omega L}\right)}{j\omega C \left(1 + \frac{G}{j\omega C}\right)}}, \tag{13}$$

$$= \sqrt{\frac{L}{C}} \left(1 + \frac{R}{j\omega L}\right)^{\frac{1}{2}} \left(1 + \frac{G}{j\omega C}\right)^{-\frac{1}{2}}. \tag{14}$$

In general, $R \ll 2\pi f L$ above a few hundred kHz. Considering cables with low-loss conductors like copper or aluminium, this relation is typically valid from about 100 kHz up to the G.fast frequency range. The relation $G \ll 2\pi f C$ is also true for most cables (especially for the ones with low-loss dielectric, e.g., polyethylene insulated). Using the assumptions of $R \ll 2\pi f L$ and $G \ll 2\pi f C$ at the frequencies of interest, we can use the following Taylor series expansions

$$\sqrt{1 + x} = 1 + \frac{x}{2} - \frac{x^2}{8} + \frac{x^3}{16} + \dots \tag{15}$$

and

$$\frac{1}{\sqrt{1 + x}} = 1 - \frac{x}{2} + \frac{3x^2}{8} - \frac{5x^3}{16} + \dots \tag{16}$$

in order to get the series expansion of (14).

The first order expansion of (14) leads to

$$Z_0 \overset{(1st)}{\approx} \sqrt{\frac{L}{C}} \left(1 - \frac{G}{2j\omega C} + \frac{R}{2j\omega L} + \frac{RG}{4\omega^2 LC}\right), \tag{17}$$

$$Z_0 \overset{(1st)}{\approx} \sqrt{\frac{L}{C}} - \frac{G}{2j\omega C}\sqrt{\frac{L}{C}} + \frac{R}{2j\omega L}\sqrt{\frac{L}{C}} + \frac{RG}{4\omega^2 LC}\sqrt{\frac{L}{C}}, \tag{18}$$

where the real and imaginary parts can be separated as

$$\Re\{Z_0\} = \sqrt{\frac{L}{C}} + \frac{RG}{4\omega^2 LC}\sqrt{\frac{L}{C}}, \tag{19}$$

and

$$\Im\{Z_0\} = \frac{G}{2\omega C}\sqrt{\frac{L}{C}} - \frac{R}{2\omega L}\sqrt{\frac{L}{C}}. \tag{20}$$

The procedure can be continued for higher orders with improved accuracy. However, the results show that the first order expansion is enough for modeling the cables of interest. So, our focus will be on modeling the terms in (19) and (20).

A key aspect of the proposed model is to verify the dependency on f for the real and imaginary parts of Z_0 ($\Re\{Z_0\}$ and $\Im\{Z_0\}$, respectively, in (19) and (20)), and combine the effect of these coefficients in a sensible way that leads to few but powerful model parameters.

First, we start with the first term of the real part, with the assumption that when $R \ll 2\pi f L$ and $G \ll 2\pi f C$, the square root term $\sqrt{L/C}$ can be assumed to be *constant* over the frequency [40]. In this case, a similar constant behavior applies for the product LC,[4] in the second part of (19).

Recalling the definition of the series resistance in the BT0$_H$ model (8), it can be seen that for high frequencies the resistance is proportional to the square root of the frequency $R \propto \sqrt{|f|}$. Similar to the reasoning presented in [14], we also adopt $G \propto |f|$ in order to describe the behavior of the shunt conductance at high frequencies. From this, we can conclude that the second term of (19) is proportional to $1/\sqrt{|f|}$, and the real part of Z_0 can be approximated by

$$\Re\{Z_0\} = h_1 + h_2 \frac{1}{\sqrt{|f|}}, \tag{21}$$

where h_1 and h_2 are two empirical parameters, that scale the *constant* term and the $1/\sqrt{|f|}$ term respectively.

The h_1 parameter can be interpreted as a value close to the mean absolute value of the characteristic impedance. Hence, a zero order approximation of Z_0 can be given by h_1 (that is, $Z_0 \approx \sqrt{L/C}$). The h_2 parameter is the parameter that controls the transition from the *low-frequency* region (that is, the region below the skin-effect mode onset [40]), to the region where the characteristic impedance tends to be constant.

Now, in order to model (20) we must focus on both accuracy and causality. First we will look at accuracy and obtain an approximation according to (20). Then we will impose restrictions to have a model for $\Im\{Z_0\}$ that corresponds to the Hilbert transform of (21).

Recalling the definition of the shunt capacitance in (12), together with the above reasoning that $G \propto |f|$ and $\sqrt{L/C}$ is constant, we can conclude that the first part of (20) can be also approximated by a *constant*. Similarly, recalling the definitions of the series resistance and series inductance in the BT0$_H$ model (8), together with the assumption that $\sqrt{L/C}$ is constant, the second part of (20) can be assumed to be proportional to $-1/\sqrt{|f|}$, and the imaginary part of Z_0 can therefore be approximated by

$$\Im\{Z_0\} = h_3 - h_4 \frac{1}{\sqrt{|f|}}, \tag{22}$$

where h_3 and h_4 are two empirical parameters, that scale the *constant* term and the $-1/\sqrt{|f|}$ term, respectively.

For the cables of interest, and at the frequencies of interest, the asymptotic value of $\Im\{Z_0\}$ tends to be zero (that is constant), due to the fact that $R \ll 2\pi f L$ and $G \ll 2\pi f C$. This behavior can be verified from cable measurements. Hence,

based on the above reasoning and in order to reduce the number of parameters for achieving a simpler model, the h_3 parameter in (22) can be set to zero.

Regarding causality, it is interesting to note that the Hilbert transform pairs $1/\sqrt{|f|} \overset{\mathcal{H}}{\rightarrow} -\mathrm{sgn}(f)/\sqrt{|f|}$ are already incorporated in the frequency dependent terms of (21) and (22). Note that $h_2 \neq h_4$ but, in order to impose causality, they can be collapsed into a single parameter. Therefore we assume $h_4 = h_2$ and $h_3 = 0$, which results in a relative small loss in accuracy in our results. Thus, the proposed model is the following.

Definition 2: The characteristic impedance, $Z_0 = \Re\{Z_0\} + j\Im\{Z_0\}$, can be modeled by

$$\Re\{Z_0\} = h_1 + h_2 \frac{1}{\sqrt{f}} \tag{23}$$

$$\Im\{Z_0\} = -h_2 \frac{1}{\sqrt{f}}. \tag{24}$$

□

In the definition we have dropped the absolute value since only positive frequencies will be used to model Z_0. The abbreviation *HM* stands for the h-model, since it is composed only by h parameters.

It should be noted that when estimating the values of h_1 and h_2, it was beneficial to include h_3 in the fitting procedure, in spite of discarding its value later on. This gives a better fitting to the imaginary part and is adopted in the next subsection.

The HM1 model has similarities with the model from the CEI/IEC [22], which is defined as follows.

Definition 3: The characteristic impedance, $Z_0 = |Z_0|e^{j\angle Z_0}$, is modeled by

$$|Z_0| = K_0 + K_1 \frac{1}{\sqrt{f}} + K_2 \frac{1}{f} + K_3 \frac{1}{\sqrt{f^3}} \tag{25}$$

$$\angle Z_0 = L_0 + L_1 \frac{1}{\sqrt{f}} + L_2 \frac{1}{f} + L_3 \frac{1}{\sqrt{f^3}}. \tag{26}$$

□

It should be noted that the CEI/IEC model is composed by $M = 8$ cable-dependent parameters ($\mathbf{\Theta} = \{K_0, K_1, K_2, K_3, L_0, L_1, L_2, L_3\}$), and it presents a non-causal behavior.[5]

C. The Analysis Procedure for the HM1 Model

As mentioned, one of the main advantages of simpler models is their potential support to simple analysis procedures. The h parameters of the HM1 model can be found via least-squares (LS) fitting from an estimated Z_0. For example, *S-parameters* measurements can be obtained at n frequency points f_i, $i = 1, \ldots, n$ using a vector network analyzer and converted to Z_0. As done in LS estimation, the squared error is minimized by imposing its partial derivatives with respect to each parameter to be zero.

---

[4]The product LC is closely related to the *phase velocity* of the line u_p, $LC = \frac{1}{u_p^2}$. For the cables of interest, when $R \ll 2\pi f L$ and $G \ll 2\pi f C$, u_p is approximately constant [40].

[5]The number of parameters of the CEI/IEC model can be reduced in order to obtain a simpler model, depending on the frequencies of interest [22]. However, the non-causality of the model is observed even when working with fewer parameters, e.g., $M = 3, 4$, or 5.

For the complex valued characteristic impedance $Z_0 = \Re\{Z_0\} + j\Im\{Z_0\}$, the squared error is given by

$$E = \sum_{i=1}^{n} \left(h_1 + h_2 \frac{1}{\sqrt{f_i}} + jh_3 - jh_2 \frac{1}{\sqrt{f_i}} \right.$$
$$\left. - \Re\{Z_0(f_i)\} - j\Im\{Z_0(f_i)\} \right)^2. \quad (27)$$

As mentioned, h_3 is included in the estimation procedure.

Taking partial derivatives with respect to each parameter of the error sum at different frequency points, and making them equal to zero, results in the following equations

$$h_1 = \frac{\sum_{i=1}^{n} \Re\{Z_0(f_i)\} - h_2 \sum_{i=1}^{n} \frac{1}{\sqrt{f_i}}}{n}, \quad (28)$$

$$h_2 = \left(\frac{\sum_{i=1}^{n} \frac{\Re\{Z_0(f_i)\}}{\sqrt{f_i}} - \sum_{i=1}^{n} \frac{\Im\{Z_0(f_i)\}}{\sqrt{f_i}}}{2 \sum_{i=1}^{n} \frac{1}{f_i}} \right.$$
$$\left. + \frac{-h_1 \sum_{i=1}^{n} \frac{1}{\sqrt{f_i}} + h_3 \sum_{i=1}^{n} \frac{1}{\sqrt{f_i}}}{2 \sum_{i=1}^{n} \frac{1}{f_i}} \right), \quad (29)$$

$$h_3 = \frac{\sum_{i=1}^{n} \Im\{Z_0(f_i)\} + h_2 \sum_{i=1}^{n} \frac{1}{\sqrt{f_i}}}{n}, \quad (30)$$

which are solved as a system of three equations and three unknowns. After influencing the values of h_1 and h_2 through the estimation procedure, the h_3 parameter is not used ($h_3 = 0$) in (24).

D. The KHM Model: Combining KM1 and HM1

To summarize, in order to compose a *complete* model for describing the secondary coefficients of the cable (γ and Z_0), the KHM model uses two equations $\Gamma = \{Z_0, \gamma\}$ and has $M = 5$ parameters.

Definition 4 (KHM): The propagation constant, $\gamma = \alpha + j\beta$, can be modeled by

$$\alpha = k_1 \sqrt{f} + k_2 f \quad (31)$$
$$\beta = k_1 \sqrt{f} - k_2 \frac{2}{\pi} f \ln f + k_3 f. \quad (32)$$

The characteristic impedance, $Z_0 = \Re\{Z_0\} + j\Im\{Z_0\}$, can be modeled by

$$\Re\{Z_0\} = h_1 + h_2 \frac{1}{\sqrt{f}} \quad (33)$$
$$\Im\{Z_0\} = -h_2 \frac{1}{\sqrt{f}}. \quad (34)$$

$\square$

In the next section the KHM model will be used in order to characterize generic G.fast copper loops, in both frequency and time domains.

V. EXPERIMENTAL RESULTS

This section discusses experiments and procedures in order to highlight the accuracy and low computational cost of the proposed KHM model when dealing with short cooper loops. Both simulated and measured data were used as references.

TABLE II
PARAMETERS OF THE KHM MODEL FITTED TO THE MEASURED CABLES

Cable/Param. (per km)	ELQXBE 50 m	ELQXBE 26 m	Cat5 62.9 m
$h1$	125.3535	126.2974	101.2393
$h2$	5.6279e+03	2.6528e+03	3.2608e+03
$k1$	0.00196	0.00175	0.00207
$k2$	4.94725e-08	5.47288e-08	2.39281e-08
$k3$	3.03643e-05	2.66477e-05	2.94153e-05

A. Experiments Using Measured Data

In the sequel, a typical *analysis* procedure is described. The goal is to obtain an estimate $\hat{\Theta}$ of the KHM model parameters from measured data Ξ.

1) Measured Cables, Used Equipments and Analysis Procedure for Obtaining $\hat{\Theta}$: The three measured cables were:

- Two Ericsson ELQXBE cables ($1 \times 4 \times 0.5$), 50 m and 26 m long;
- One Typical Cat5 cable ($4 \times 2 \times 0.5$), 62.9 m long.

A typical Cat5 and Ericsson ELQXBE cables were adopted in this work since they represent copper cables with physical properties (e.g., diameter and arrangement of the wires, insulation, etc.) that are similar to the ones described for the lines that compose the *In-home* sections of some G.fast reference topologies [15].

The Ericsson ELQXBE is an indoor cable developed for telecommunication systems, e.g., for xDSL and POTS (plain old telephone service) transmission. It is polyethylene insulated, jacketed with a halogen-free thermoplastic compound, and the wires are twisted into a star quad composed by two pairs. The typical Cat5 is a common cable used in structured cabling for computer networks, such as Ethernet.

The *S-parameters* of one pair within the cited cables were measured in a frequency range from 100 kHz up to 212 MHz using an Agilent E5071C Network Analyzer. The corresponding characteristic impedances and propagation constants were estimated from the measurements, and they were used in the analysis procedure based on the equations discussed in Section IV-C and [14] in order to obtain the values for the h and k parameters that best fit Ξ. Table II shows the estimated parameters.

2) Modeling Single Segments: Using the estimated set $\hat{\Theta}$ of parameters presented in Table II and the synthesis equations of the KHM model, the following quantities were derived for each cable segment: the secondary coefficients, input impedances, transfer functions and impulse responses.

Fig. 1 shows the measured and modeled absolute values for the characteristic impedances. The characteristic impedance curves from the Ericsson ELQXBE 26 m cable are omitted in Fig. 1 due to their similarity with the ones derived from the Ericsson ELQXBE 50 m cable.

Fig. 2 shows the measured and modeled absolute values for the transfer functions. The modeled transfer functions were obtained using an equivalent representation as an ABCD matrix, composed by the modeled Z_0 and γ.

Similarly, Figs. 3 and 4 show the measured and modeled absolute values for the open and short circuit input impedances of the Cat5 pair. The results obtained using the KHM model are
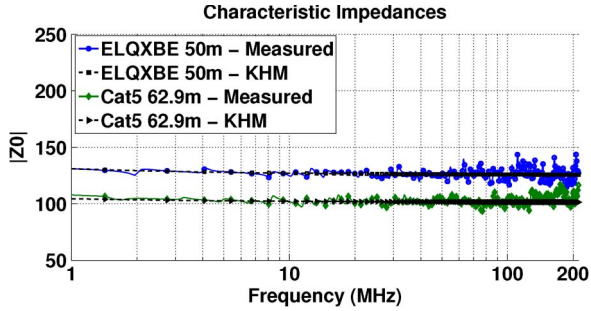
Fig. 1.   Measured and modeled absolute values for the characteristic impedances.
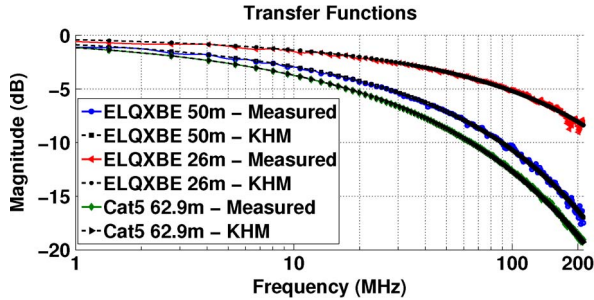

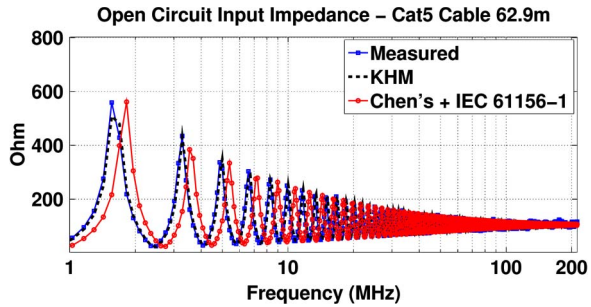Fig. 2.   Measured and modeled absolute values for the transfer functions.

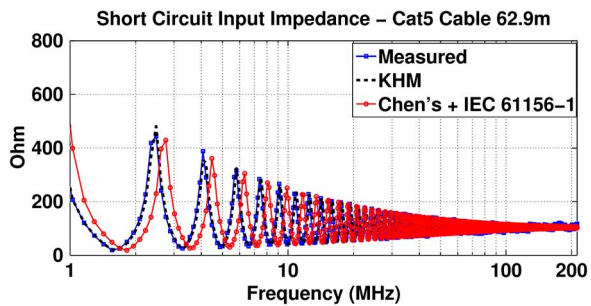Fig. 3.   Measured and modeled open circuit input impedances for the Cat5 pair.

Fig. 4.   Measured and modeled short circuit input impedances for the Cat5 pair.

compared with the ones obtained when Z_0 is modeled using the CEI/IEC [22] and γ is modeled using Chen's model [8]. The objective here is to contrast the results given by the KHM with the ones given by other simplified models present in the literature.

While the models were somehow equivalent in frequency-domain, the same was not observed in time-domain. Considering the Cat5 cable, the propagation delay was estimated approximately as $T_{pd} = 280$ ns. From Fig. 5, it is possible to observe that the causality in the impulse response is preserved only when the KHM model is used (since it obeys the minimum required time imposed by the propagation delay). The impulse
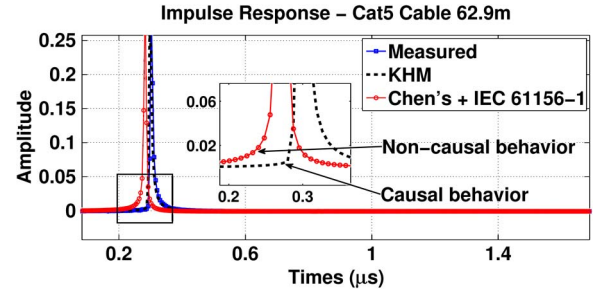

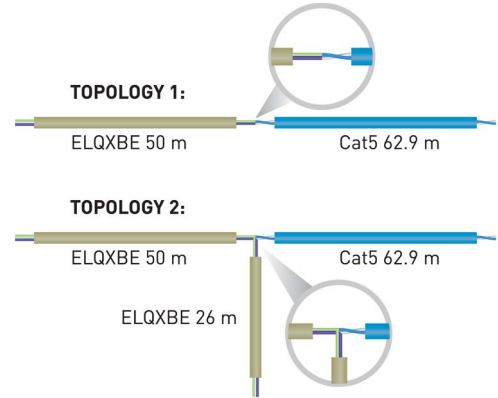Fig. 5.   Measured and modeled impulse responses for the Cat5 pair.

Fig. 6.   The two generic loops that were measured and modeled.

responses were derived by the inverse Fourier transform of the frequency responses.

3) Modeling Multiple Segments: Beyond working with single cable segments, the KHM model was also tested for modeling copper loops containing multiple segments. For this purpose, two generic loops were defined using the previously measured cables: one loop containing two segments in series and the other containing two segments in series with one bridged-tap, composing two distinct topologies:

- Topology 1: ELQXBE cable 50 m + Cat5 cable 62.9 m in series;
- Topology 2: ELQXBE cable 50 m + Cat5 cable 62.9 m in series + ELQXBE cable 26 m as shunt bridged-tap.

Measurements of the two topologies were obtained by combining the cable segments as indicated in Fig. 6.

The derived transfer functions and impulse responses were compared with the ones obtained using the proposed model. The modeled transfer functions were calculated using an equivalent ABCD matrix composed by the product of the individual ABCD matrices of each segment, which were derived using the corresponding set of estimated parameters $\hat{\Theta}$ from Table II, and the synthesis equations of the KHM model.

Figs. 7 and 8 show the results for Topology 1, and Figs. 9 and 10 show the results for Topology 2.

B. Validating the Model Using Simulated G.fast Topologies

Beyond fitting measurements, the KHM model was also tested using simulated data that characterizes three G.fast reference topologies [15]. The G.fast reference topologies describe copper loop configurations expected to be found in real G.fast deployments.
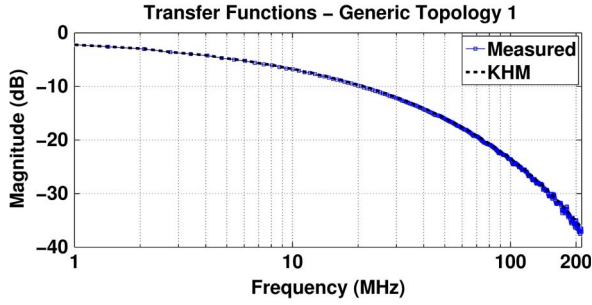
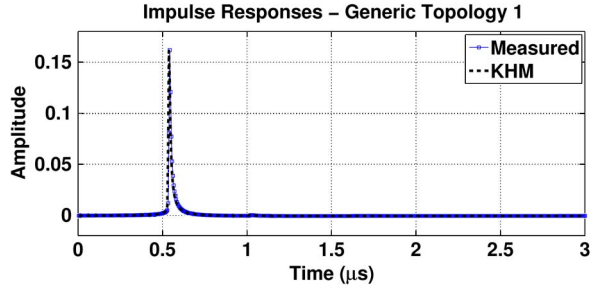Fig. 7. Measured and modeled transfer functions for topology 1.

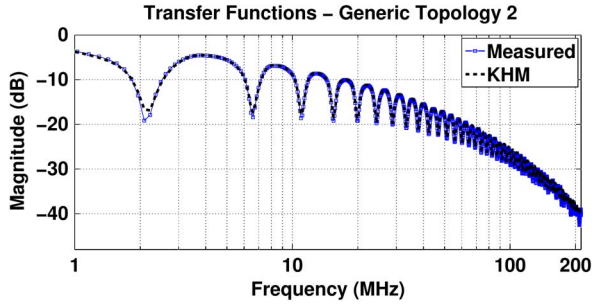Fig. 8. Measured and modeled impulse responses for topology 1.

Fig. 9. Measured and modeled transfer functions for topology 2.
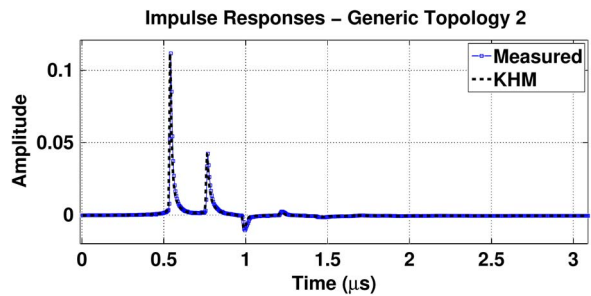

Fig. 10. Measured and modeled impulse responses for topology 2.

In our experiments, three reference combinations of a final drop loop and an in-premises wiring were selected from [15]: D3-H5, D4-H5, and D4-H3, composed primarily by CAD55 cables. For completeness, the chosen topologies are described in the Appendix, together with the associated cable model and parameters for simulation purposes.

In order to obtain the results, first, we use the reference model, synthesis equations and set Θ of parameters defined by the ITU in [15] in order to obtain by simulation the primary and secondary coefficients of the CAD55 cables. The simulation was performed using a frequency range from 100 kHz up to 212 MHz. Using the data Ξ from these simulations, an analysis

TABLE III
PARAMETERS OF THE KHM MODEL FITTED TO THE CAD55 CABLE

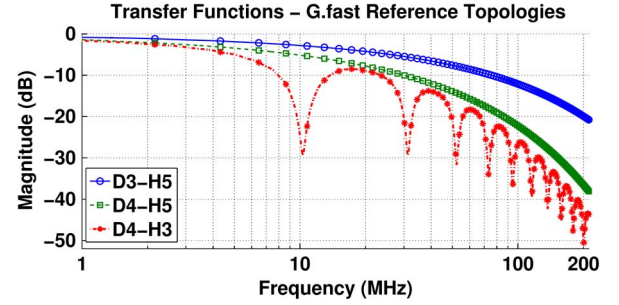| Param. (per km)	Value
$h1$	106.5050
$h2$	5.9318e+03
$k1$	0.00185
$k2$	1.20594e-07
$k3$	3.11222e-05

Fig. 11. Transfer functions of the three G.fast reference topologies as modeled by KHM.
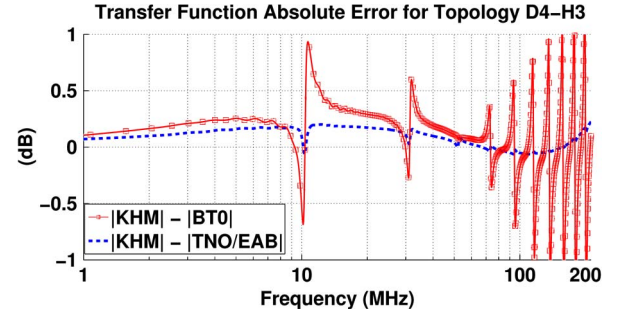

Fig. 12. Absolute error (difference) in dB between modeled transfer functions for the topology D4-H3.

procedure was performed in order to obtain estimates $\hat{\Theta}$ of the values for the h and k parameters that best fit the CAD55 cables. Table III shows the results.

After obtaining the set $\hat{\Theta}$ of parameters from Table III and using the KHM synthesis equations, the ABCD matrix of each segment was derived. The transfer functions of the whole topologies were then obtained by cascading the individual sections (such as in Section V-A3). Fig. 11 shows the transfer functions of the three analyzed G.fast reference topologies, as modeled by KHM.

The accuracy of the proposed model is illustrated in Fig. 12, that shows the transfer function absolute error in dB, derived when modeling the topology D4-H3 using the KHM model, the cable model currently adopted by ITU (TNO/EAB model) and the non-causal BT0 model. The synthesis equations and set Θ of parameters for describing CAD55 cables using the BT0 model [41] are given in the Appendix. It was noted a maximum error of approximately 1 dB when considering the frequency range up to 212 MHz.

In order to compare the impact of eventual discrepancies in simulation results obtained using these three models, bit rate estimates were performed using the derived transfer functions for the loop D4-H3. The assumptions for the simulations are shown in Table IV, and the results are presented in Table V. The numbers indicate that all three models led to equivalent results

TABLE IV
ASSUMPTIONS FOR THE BIT RATE SIMULATIONS

Parameter	Value
Transmit PSD	flat,-76 dBm/Hz
Background noise	AWGN, -140 dBm/Hz
Margin	6 dB
Coding gain	5 dB
SNR gap Γ	9.75 dB
Max bit load	12
Min bit load	1
Start frequencies	2.2 MHz, 12 MHz, 17.7 MHz, 30 MHz
Upper frequency	106 MHz
Carrier spacing	48.8 kHz
$Z_s = Z_l$	100 Ohms
Transmission efficiency	90%
Crosstalk	The crosstalk was not considered

TABLE V
BIT RATE ESTIMATION IN Mb/s FOR THE D4-H3 TOPOLOGY,
USING VARIOUS START FREQUENCIES AND CHANNEL MODELS

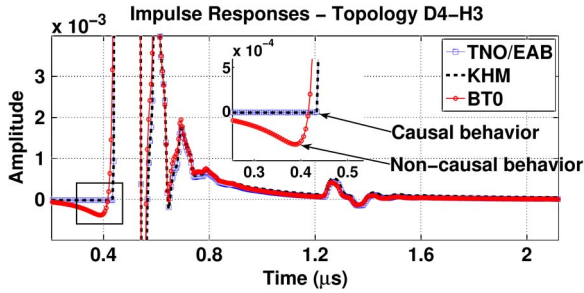| Start frequency	TNO/EAB model	KHM model	BT0 model
2.2 MHz	984	984	984
12 MHz	881	881	881
17.7 MHz	820	820	819
30 MHz	687	687	687

Fig. 13. Impulse response of the topology D4-H3 modeled by the KHM, TNO/EAB and BT0 models.

in these frequency-domain simulations. The same behavior was observed for the other G.fast topologies.

Targeting time-domain simulations, Fig. 13 shows the impulse responses of the loop D4-H3 modeled by the KHM, TNO/EAB and BT0 models. As expected, it is possible to observe a non-causal behavior when using the BT0 model while the impulse responses obtained with KHM and TNO/EAB are causal.

Considering that KHM and TNO/EAB are equivalent in terms of accuracy in both frequency and time domains for the tested G.fast topologies, it is of interest to compare their computational cost.

C. On the Computational Cost of KHM

One of the main advantages of the proposed model when compared with more sophisticated models is related to its reduced computational cost when performing both analysis and synthesis procedures.

Because benchmarks are complex to setup and dependent on several factors such as the target computing platform, two evaluation methods are discussed in the sequence, which are

TABLE VI
THE NUMBER Q_{op} OF OPERATIONS WITH ASSOCIATED CCI
FOR EACH MODEL, AND THE ASSOCIATED WEIGHT P_{op}

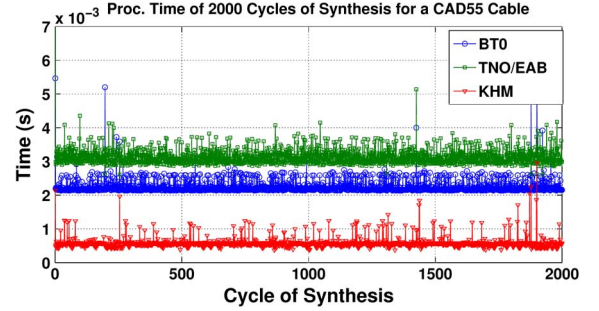|	BT0	TNO/EAB	KHM	P_{op}
Add ($+$)	12	7	5	1
Sub ($-$)	-	2	1	1
Mult ($*$)	25	57	11	1
Div ($\div$)	7	15	3	1
Sqrt ($\sqrt{x}$)	2	3	4	10.35
Log ($\ln x$)	-	-	1	36.5
Pow (x^y)	14	12	-	74.35
CCI	1105.6	1995.8	97.9	

Fig. 14. Processing time of 2000 synthesis procedures using the BT0, TNO/EAB and KHM models for modeling a single segment of CAD55 cable.

TABLE VII
AVERAGE TIME, STANDARD DEVIATION AND TOTAL TIME SPENT BY
EACH MODEL TO FINISH THE 2000 SYNTHESIS OPERATIONS

	BT0 [4]	TNO/EAB [13]	KHM
Total time (s)	4.4927	6.2630	1.1509
Average time (s)	2.2463e-003	3.1314e-003	5.7543e-004
Std. deviation (s)	2.0875e-004	2.8789e-004	1.5303e-004

complementary and can provide an idea about the involved computational cost.

First, we compare the KHM, TNO/EAB, and BT0 models using a complexity index, similar to the one proposed in [42]. The computational complexity index (CCI) is based on the assignment of relative weights for every mathematical operation, and is given as

$$\text{CCI} = \sum_{op} Q_{op} P_{op}, \qquad (35)$$

where op is the operation, Q_{op} is the number of occurrences of the operation and P_{op} its corresponding weight.

The CCI associated to each model was calculated by using their synthesis equations and parameters in order to derive the complex values of Z_0 and γ for an arbitrary frequency point f. The number of necessary operations as well as the resulting CCI are shown in Table VI. The weights, which are platform-dependent as mentioned, were tuned here for modern Pentium CPUs after extensive tests with the GCC compiler.

To complement the CCI results, computing times were compared with the models implemented in MATLAB. These numbers were obtained using native functions from MATLAB running on an Intel Core i5 processor.

Fig. 14 illustrates the processing time of 2000 *runs of synthesis* using the parameters and equations of the KHM, TNO/EAB and BT0 models for modeling a single segment of CAD55
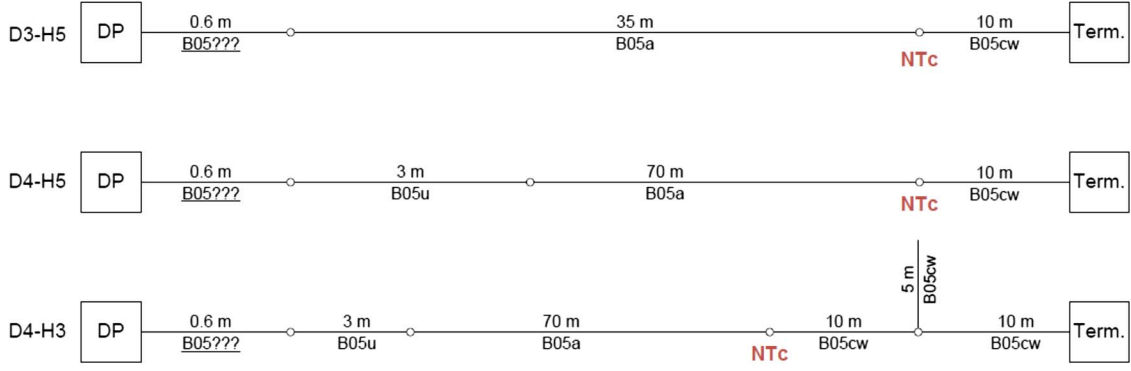
Fig. 15. The three G.fast reference loops simulated (from [15]).

cable. The parameter values for the BT0 and TNO/EAB models where set as in [41] (see Appendix). The parameters values for the KHM model were set as in Table III. The frequency range adopted for simulation was from 2.2 MHz to 106 MHz.

Table VII presents the total time spent by each model for the 2000 synthesis procedures, as well as the average time and standard deviation.

In this simple test, the synthesis procedure of the proposed model proved to be considerably faster than the two baselines. In applications such as [27], which performs loop topology identification by invoking the adopted model synthesis procedure approximately 300 to 2000 times (depending on the topology) within its analysis-by-synthesis search, the reduction in the total time may be significant.

This discussion emphasized the synthesis procedure, but the KHM model is also competitive with respect to the computational cost of its analysis procedure due to the closed-form expressions.

VI. CONCLUSION

This work presented a causal model with only 5 parameters for the characteristic impedance and propagation constant of twisted-pair cables. The so-called KHM model is valid for frequencies up to a couple of hundred MHz and has a closed-form expression for fitting the model parameters to measured data during the analysis process. The proposed model can be adopted in applications that work in frequency domain and also those in time domain. The experimental results indicated that the model can be potentially used for modeling single segments or an arbitrary topology with multiple segments of distinct gauges connected in cascade and with bridged-taps, presenting good accuracy for G.fast topologies with low complexity.

APPENDIX

This Appendix presents the three G.fast reference loops simulated in Section V-B, which are illustrated in Fig. 15. These three loops were selected in order to avoid scenarios composed by cables of type *A26j*, *A24u* or *CAT-3* in [15], which were not completely specified yet.

The cable model and parameters adopted by the ITU in order to simulate the electric characteristics of CAD55 cables are given in Definition 5 and in Table VIII [15] respectively.

TABLE VIII
PARAMETERS FOR THE CABLE TYPE CAD55 (FROM [15])

Param.	Value
$Z_{0\infty}$	105.0694
η_{VF}	0.6976
R_{s0}	0.1871
q_L	1.5315
q_H	0.7415
q_x	1
q_y	0
q_c	1.0016
ϕ	-0.2356
f_d	1.000000

TABLE IX
PARAMETERS FOR THE CABLE TYPE CAD55 (FROM [41])

Param.	Value
R_{oc}	187.0831
a_c	0.0457
L_0	6.5553e-004
L_∞	5.0973e-004
f_m	8.1241e+005
Nb	1.0142
g_0	1.0486e-010
N_{ge}	1.1500
C_0	-6.9514e-011
C_∞	4.5578e-008
N_{ce}	-0.1500

Furthermore, the synthesis equations for the BT0 model are given in Definition 6 and the parameters for describing CAD55 cables using this model are given in Table IX [41].

Definition 5 (TNO/EAB): The primary coefficients are given by

$$Z(f) = j2\pi f L_\infty + R_{s0}\left(1 - q_s.q_x\right.$$

$$\left. + \sqrt{q_s^2 \cdot q_x^2 + 2\frac{j2\pi f}{\omega_s} \cdot \left(\frac{q_s^2 + \frac{j2\pi f}{\omega_s} \cdot q_y}{\frac{q_s^2}{q_x} + \frac{j2\pi f}{\omega_s} \cdot q_y}\right)}\right), \quad (36)$$

$$Y(f) = j2\pi f C_{p0} \times (1 - q_c) \times \left(1 + \frac{j2\pi f}{\omega_d}\right)^{\frac{-2\phi}{\pi}}$$

$$+ j2\pi f C_{p0} \times q_c, \quad (37)$$

where

$$L_{s\infty} = \frac{1}{\eta_{VF} \times c_0} Z_{0\infty}, \tag{38}$$

$$C_{p0} = \frac{1}{\eta_{VF}.c_0} \times \frac{1}{Z_{0\infty}}, \tag{39}$$

$$q_s = \frac{1}{q_H^2.q_L}, \tag{40}$$

$$\omega_s = q_H^2.j2\pi f_{s0} = q_H^2.\left(\frac{4\pi.R_{s0}}{\mu_0}\right), \tag{41}$$

$$\omega_d = 2\pi f_d. \tag{42}$$

$\square$

Definition 6 (BT0): The primary coefficients are given by

$$R(f) = \sqrt[4]{R_{oc}^4 + a_c f^2}, \tag{43}$$

$$L(f) = \frac{L_0 + L_\infty \left(\frac{f}{f_m}\right)^{Nb}}{1 + \left(\frac{f}{f_m}\right)^{Nb}}, \tag{44}$$

$$C(f) = C_\infty + C_0 f^{-N_{ce}}, \tag{45}$$

$$G(f) = g_0 f^{N_{ge}}. \tag{46}$$

$\square$

ACKNOWLEDGMENT

REFERENCES

[1] J. Bourne, "Fiber to the home: Practically a reality," in *Conf. Rec. IEEE ICC Digit. Technol.—Spanning Universe*, 1988, vol. 2, pp. 890–894.

[2] P. Ödling *et al.*, "The fourth generation broadband concept," *IEEE Commun. Mag.*, vol. 47, no. 1, pp. 62–69, Jan. 2009.

[3] M. Timmers, M. Guenach, C. Nuzman, and J. Maes, "G.fast: Evolving the copper access network," *IEEE Commun. Mag.*, vol. 51, no. 8, pp. 74–79, Aug. 2013.

[4] BT, "Parametric modeling of twisted pair cables for VDSL," ANSI contribution, T1E1.4/96-15, Jan. 1996.

[5] "VDSL—Measurements and models on Dutch cables," Leidschendam, The Netherlands, ETSI STC TM6 Contribution TD15, [t15r0], Mar. 1997.

[6] R. F. M. Van Den Brink, "Cable reference models for simulating metallic access networks," Eur. Telecommun. Standards Inst. (ETSI), Sophia-Antipolis Cedex, France, ETSI STC TM6, Permanent Document TM6(97)02, Jun. 1998.

[7] J. Musson, "Maximum Likelihood estimation of the primary parameters of twisted pair cables," Eur. Telecommun. Standards Inst. (ETSI), Sophia-Antipolis Cedex, France, ETSI STC TM6 Contribution TD8, [t08a0], Jan. 1998.

[8] W. Y. Chen, *DSL: Simulation Techniques and Standards Development for Digital Subscriber Lines*. Indianapolis, IN, USA: Macmillan, 1998.

[9] P. Boets, M. Zekri, L. Van Biesen, T. Bostoen, and T. Pollet, "On the identification of cables for metallic access networks," in *Proc. 18th IEEE IMTC*, vol. 2, pp. 1348–1353.

[10] T. Bostoen *et al.*, "Estimation of the transfer function of a subscriber loop by means of a one-port scattering parameter measurement at the central office," *IEEE J. Sel. Areas Commun.*, vol. 20, no. 5, pp. 936–948, Jun. 2002.

[11] F. Lindqvist *et al.*, "Low-order and causal twisted-pair cable modeling by means of the Hilbert transform," in *Proc. RVK08—20th Nordic Conf. Radio Sci. Commun.*, 2008, vol. 1106, pp. 301–310, AIP Conference Proceeding.

[12] "G.fast: Wideband modeling of twisted pair cables as two-ports," Delft, The Netherlands, ITU-T contribution, Temporary Document 11GS3-028, Sep. 2011.

[13] Ericsson AB and TNO, "Improved model for shunt admittance in G.fast cable mode," ITU-T contribution, temporary document 2012-05-4A-045, May 2012.

[14] D. Acatauassu *et al.*, "Simple and causal twisted-pair channel models for G.fast systems," in *Proc. IEEE GLOBECOM*, Dec. 2013, pp. 2834–2839.

[15] Associate Rapporteur for G.fast, "Updated draft text for G.fast—Version 10.0," ITU-T contribution, temporary document 2013-12-Q4-R20, Dec. 2013.

[16] BT, ITU-T Contribution, Temporary Document 11RV-026R2 G.fast: Cable Models, Oct. 2011 ITU-T Contribution, Temporary Document 11RV-026R2.

[17] D. M. Pozar, *Microwave Engineering*, 2nd ed. New York, NY, USA: Wiley, 1998.

[18] T. Starr, J. M. Cioffi, and P. J. Silverman, *Understanding Digital Subscriber Line Technology*. Englewood Cliffs, NJ, USA: Prentice-Hall, 1999.

[19] P. Golden, H. Dedieu, and K. Jacobsen, *Fundamentals of DSL Technology*. New York, NY, USA: Auerbach, 2006.

[20] S.-W. Wei, "Simple RLCG model for category-5 cables," *Electron. Lett.*, vol. 33, no. 25, pp. 2108–2109, Dec. 1997.

[21] TIA/EIA, "TIA/EIA Standard—Comercial Building Telecommunications Cabling Standard," Part 2: Balannced Twisted-Pair Cabling Components, TIA/EIA-568-B.2, May 2001.

[22] CEI/IEC, "CEI/IEC International Standard," Multicore and symmetrical pair/quad cables for digital communications—Part 1: Generic specification, CEI/IEC 61156-1, Dec. 2002.

[23] P. Boets and L. V. Biesen, "Metallic 2-wire Parametric Line Models—A Survey," in *Proc. 18th Imeko World Congr.*, 2006, pp. 1–6.

[24] D. E. Goldberg, *Genetic Algorithms in Search, Optimization and Machine Learning*. Reading, MA, USA: Addison-Wesley, 1989.

[25] R. Pintelon, P. Guillaume, Y. Rolain, J. Schoukens, and H. Van Hamme, "Parametric identification of transfer functions in the frequency domain—A survey," *IEEE Trans. Autom. Control*, vol. 39, no. 11, pp. 2245–2260, Nov. 1994.

[26] R. M. Rodrigues, C. Sales, A. Klautau, K. Ericson, and J. Costa, "Transfer function estimation of telephone lines from input impedance measurements," *IEEE Trans. Instrum. Meas.*, vol. 61, no. 1, pp. 43–54, Jan. 2012.

[27] C. Sales *et al.*, "Line topology identification using multiobjective evolutionary computation," *IEEE Trans. Instrum. Meas.*, vol. 59, no. 3, pp. 715–729, Mar. 2010.

[28] T. Magesacher *et al.*, "Measurement and modeling of short copper cables for ultra-wideband communication," in *Proc. SPIE Opt. East Broadband Access Commun. Technol.*, Oct. 2006, vol. 6390, p. 39006.

[29] L. Heylen and J. Musson, "Cable models predict physically impossible behaviour in time domain," *ETSI TM6 contribution TD53, [t53a0]*, Nov. 1999.

[30] W. Henkel, G. Tauböck, P. Ödling, P. O. Börjesson, and N. Petersson, "The cyclic prefix of OFDM/DMT—An analysis," in *Proc. Int. Zurich Seminar Broadband Commun. Access, Transmiss., Netw.*, 2002, pp. 22-1–22-3.

[31] C. Valenti, "NEXT and FEXT models for twisted-pair North American loop plant," *IEEE J. Sel. Areas Commun.*, vol. 20, no. 5, pp. 893–900, Jun. 2002.

[32] "Transmission and multiplexing (TM); Access networks spectral management on metallic access networks; Part 2: Technical methods for performance evaluations," Sophia-Antipolis Cedex, France, ETSI TR 101 830-2, Jul. 2008.

[33] *American National Standard for Telecommunications—Spectrum Management for Loop Transmission Systems*, ANSI Standard T1.417, Sep. 2003.

[34] J.-J. Werner, "The HDSL environment [high bit rate digital subscriber line]," *IEEE J. Sel. Areas Commun.*, vol. 9, no. 6, pp. 785–800, Aug. 1991.

[35] M. Sorbara, P. Duvaut, F. Shmulyian, S. Singh, and A. Mahadevan, "Construction of a DSL-MIMO channel model for evaluation of FEXT cancellation systems in VDSL2," in *Proc. IEEE Sarnoff Symp.*, Apr 2007, pp. 1–6.

[36] J. Maes, M. Guenach, and M. Peeters, "Statistical MIMO channel model for gain quantification of DSL crosstalk mitigation techniques," in *Proc. IEEE ICC*, Jun. 2009, pp. 1–5.

[37] "G.fast: Far-end crosstalk in twisted pair cabling; measurements and modelling," ITU-T Contribution, Temporary Document 11RV-022, Nov. 2011.

[38] "G.fast: Dual slope behaviour of EL-FEXT," Delft, The Netherlands, ITU-T Contribution, Temporary Document 2012-02-4A-038, Feb. 2012.

[39] E. Bogatin, *Signal Integrity—Simplified*. Upper Saddle River, NJ, USA: Prentice-Hall, 2003.

[40] H. Johnson and M. Graham, *High-Speed Signal Propagation: Advanced Black Magic*. Upper Saddle River, NJ, USA: Prentice-Hall, 2003.

[41] "G.fast: Updated measurements and modelling of CAD55 cable," Kista, Sweden, ITU-T Contribution, COM 15—C 2352—E, Aug. 2012.

[42] J. R. B. De Marca, "An LSF quantizer for the North-American half-rate speech coder," *IEEE Trans. Veh. Technol.*, vol. 43, no. 3, pp. 413–419, Aug. 1994.

Diogo Acatauassu (M'08) was born in Belém, Brazil, in 1983. He received the B.S. degree in computer engineering and the M.Sc. degree in electrical engineering from the Federal University of Pará (UFPA), Belém, Brazil, in 2006 and 2009, respectively, where he is currently working toward the Ph.D. degree in electrical enginerring.

Since 2006, he has been with the Signal Processing Laboratory (LaPS), Belém. In the fall of 2011, he was a Visiting Researcher with the Ericsson Research, Stockholm, Sweden. His current research interests are in the fields of measurements, modeling, and noise mitigation techniques applied to copper-based transmission technologies.

Miguel Berg (S'95–M'03) was born in Sundsvall, Sweden, in 1968. He received the B.S. degree in electrical engineering from Mid Sweden University, Sundsvall, in 1995 and the Lic. degree and the Ph.D. degree in wireless communication systems from the Royal Institute of Technology, Stockholm, Sweden, in 1999 and 2002, respectively.

From 2002 to 2003, he was an Engineer with Radio Components Sweden AB, Stockholm. During 2004–2006, he was a Researcher with the Royal Institute of Technology and, during 2006–2007, with Lund University, Lund, Sweden, working mainly with DSL line testing. In May 2007, he joined Ericsson AB, Stockholm, where he is currently a Master Researcher. He has coauthored about 20 peer-reviewed publications and filed more than 30 patent applications. His current research interests include copper-based communication and small-cell wireless communication systems.

Stefan Höst (S'95–M'00) was born in Malmö, Sweden, in 1968. He received the M.Sc. degree in computer science and the Ph.D. degree in information theory from Lund University, Lund, Sweden, in 1994 and 2000, respectively.

In February 2000, he became an Associate Professor with the Department of Electrical and Information Technology, Lund University. His research interests are mainly communication systems, information theory, and signal processing. He is particularly active in the access part of the network, working with both fixed and mobile access to the end user.

Aldebaro Klautau (S'92–M'97–SM'08) received the Ph.D. degree from the University of California, San Diego, CA, USA, in 2003.

In 1995, he was a Faculty Member with the Federal University of Santa Catarina, Florianópolis, Brazil. Since 1996, he has been with the Federal University of Pará (UFPA), Belém, Brazil, affiliated with the Computer Science (PPGCC) and Electrical Engineering (PPGEE) Graduate Programs. At UFPA, he is currently the ITU-T TIES Focal Point and directs the Signal Processing (LaPS) and the Embedded Systems (LASSE) research groups. His work focuses on signal processing and machine learning applied to telecommunications. He is a Researcher of the Brazilian National Council of Scientific and Technological Development (CNPq).

Chenguang Lu was born in Henan province, China, in 1978. He received the M.Sc. degree in digital communication from Chalmers University of Technology, Gothenburg, Sweden, in 2005 and the Ph.D. degree in wireless communication from Aalborg University, Aalborg, Denmark, in 2008.

In 2008, he was a Visiting Scholar with the University of Illinois at Urbana–Champaign, Champaign, IL, USA. Since 2008, he has been with Ericsson Research, Stockholm, Sweden, where he has been mainly doing research on fixed-access network and small-cell transport. He is currently a Senior Researcher with Ericsson Research. He has coauthored over ten publications in peer-reviewed conferences and journals and has filed over 40 patent applications.

Per Ola Börjesson (SM'01) received the Ph.D. and Docent degree in telecommunication theory from Lund University, Lund, Sweden, in 1980 and 1983, respectively.

Between 1988 and 1998, he was a Professor of signal processing with Luleå University of Technology, Luleå, Sweden. Since 1998, he has been a Professor of signal processing with Lund University. He is currently researching loop qualification and orthogonal frequency-division multiplexing (OFDM) or discrete multitone modulation at Ericsson Research with Broadband Technologies Network Management and Mobile Backhaul. He has filed about 25 patents and has published more than 60 original refereed scientific papers and conference papers, among them are highly cited works concerning synchronization and channel estimation for OFDM systems. His primary research interests focus on various issues related to high-performance communication systems, particularly high-data-rate wireless and twisted-pair systems. He emphasizes the interaction between models and real systems, from the creation of application-oriented models based on system knowledge to the implementation and evaluation of algorithms.